九州大学学術情報リポジトリ
Kyushu University Institutional Repository

Magnetotelluric Soundings in Minami-Noshiro Oil Field, Japan

Khalil, Ahmed
Department of Earth Resources Engineering : Graduate Student

Ushijima, Keisuke
Department of Earth Resources Engineering : Professor

https://hdl.handle.net/2324/1130

出版情報：九州大学工学紀要. 63 (2), pp.87-106, 2003-06-26. 九州大学大学院工学研究院
バージョン：
権利関係：

KYUSHU UNIVERSITY

Memoirs of the Faculty of Engineering, Kyushu University, Vol. 63, No. 2, June 2003

Magnetotelluric Soundings in Minami-Noshiro Oil Field, Japan

by

Ahmed KHALIL* and Keisuke USHIJIMA**

(Received March 25, 2003)

Abstract

In 1997-1998, a three-dimensional MT survey has been carried out over a volcanic area in Japan called Minami-Noshiro by Japan National Oil Corporation. Minami-Noshiro area is located in the northern part of Akita prefecture, northeastern Japan and represents the northwestern margin of the Akita oil field. This paper demonstrates the application of magnetotelluric (MT) method for hydrocarbon exploration to determine the subsurface electrical resistivity structure in this area. In particular, results of analysis of the impedance tensor, which describes the relationship between the electric, and the magnetic field components are presented. Moreover, results of advanced interpretation techniques of one-dimensional (1-D) and two-dimensional (2-D) inversions are documented. Processing and analysis of impedance tensor of the magnetotelluric data revealed a regional strike of N30°E and high conductive zones distribute at lower crustal levels beneath the study area. Also, one-dimensional inversion of the invariants at each site indicates that a number of low-resistivity zones exist in the sedimentary formations. As well as, there is a good agreement between the results of 1-D models and well logging data. Interpretation of the geomagnetic transfer functions was also made in terms of a two-dimensional inversion of TE (transverse electric) and TM (transverse magnetic) resistivity along three W-E profiles (lines 400, 500 and 900). These lines are parallel to the geologic section in the study area. The results obtained from two-dimensional inversions indicate that high conductive zones are detected at different levels of the resistivity sections with various thicknesses from west to east.

Keywords: Magnetotelluric (MT) method, Minami-Noshiro oil field, 1-D and 2-D inversions, Well logging data, Electrical resistivity structure

1. Introduction

Measurements of the earth's natural electric and magnetic fields are used to infer the subsurface electrical resistivity that can be related to rock units. Also, rotational invariants of the magnetotelluric (MT) impedance tensor have long been used to provide information about the underlying geoelectric structure. Well-known examples are the Berdichevsky and

* Graduate Student, Department of Earth Resources Engineering
** Professor, Department of Earth Resources Engineering

determinant impedances [3,20,10,17], which were introduced to represent in some sense an 'average impedance' from which a 1-D interpretation of the structure could be deduced. The MT method is a common technique for imaging deep electrical structure because it has capability to detect high conductive zones and it is able to image structures from a few tens of meters to hundreds of kilometers into the earth. In the simplest situation one may consider the Earth as a uniform half-space, or as a horizontally layered (1-D). More complicated structures are 2-D, when the resistivity varies with depth, as well as one horizontal direction (perpendicular to what might then be called the geological strike), or 3-D in the most general situation. Minami-Noshiro area is located in the northern part of Akita prefecture and represents the northwestern margin of the Akita oil field as shown in **Fig. 1**. In 1997-1998, a

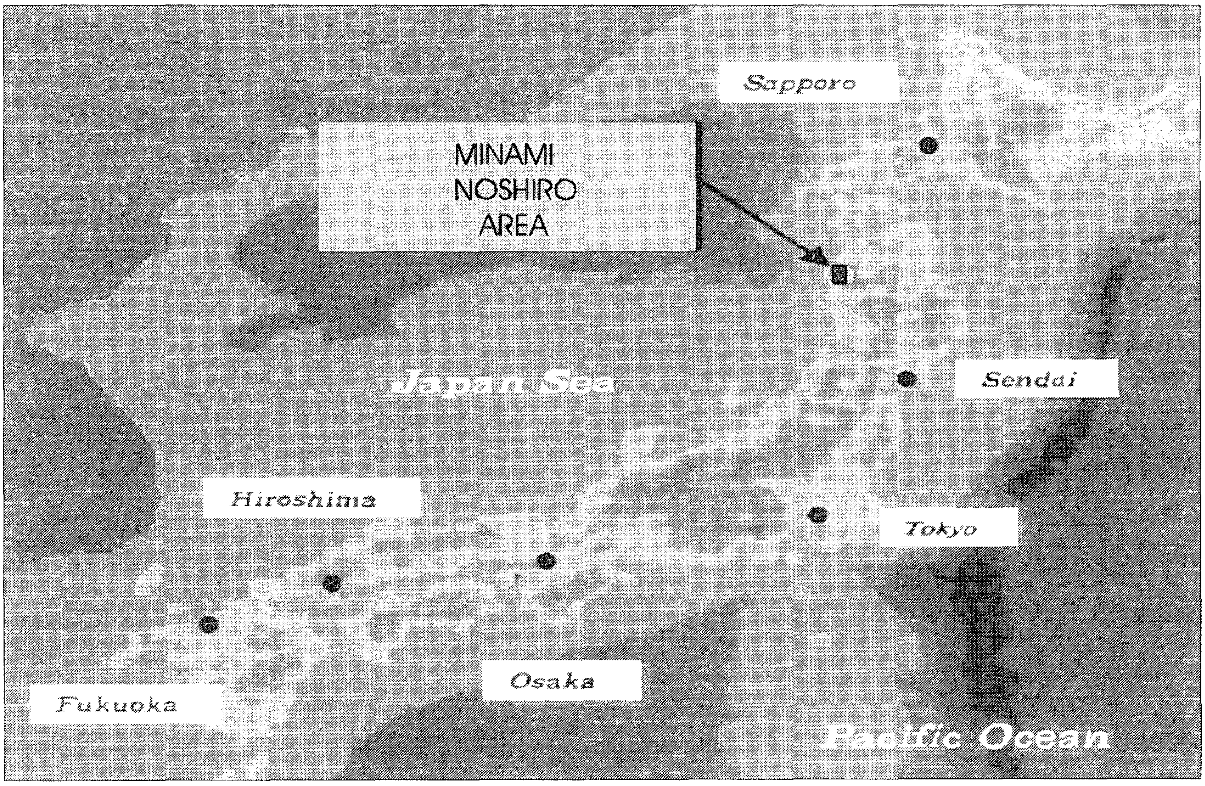

Fig. 1 Location map of Minami-Noshiro area.

three-dimensional MT survey was conducted in Minami-Noshiro area by Japan National Oil Corporation (JNOC). The Satellite Synchronized MT system (manufactured by Phoenix Geophysics) was used. The MT remote reference surveys have been carried out by Nittetsu Mining Company retained by JNOC to acquire 195 MT soundings over 40 km^2. The MT survey was conducted along nine east-west lines as shown in **Fig. 2**. The remote reference site was about 100 km away from the survey area. A conventional MT survey acquired time-series data for five components at each site. The time-series data between each local site and the remote reference site was synchronized using a high precision clock. Conventional surveys involve difficulties in getting places to set the systems, especially when survey area is close to population centers or cultivated lands. The frequency range of the observed data is from 320 Hz to 0.0055 Hz. Measurement sites for the in-line direction were separated by 250-500 m at the center of the survey area and 1000 m at the either end of a survey line. Cross-lines are separated by 500 m.

The purpose of this study is to determine the deeper structure in Minami-Noshiro oil field based on advanced analysis of the observed MT data. The MT data were processed using

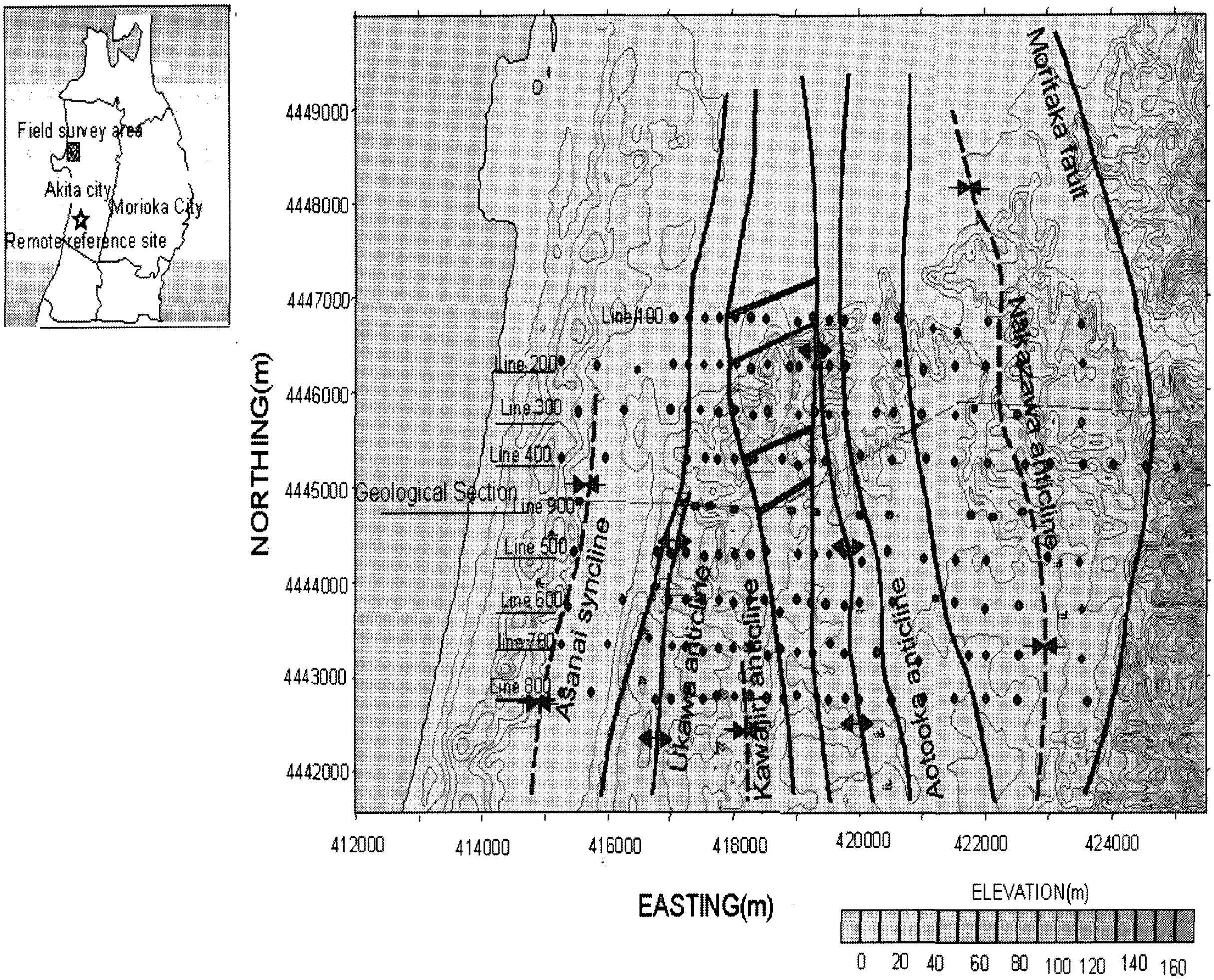

Fig. 2 Location of MT survey sites on a topographic map of the study area.

Geotools software, the resulting impedance tensor elements were used to compute the apparent resistivities and phases, then, 1-D Occam and Marquardt inversions were applied to the calculated apparent resistivities to construct the actual resistivity of the subsurface structure. We obtained the pseudosections of apparent resistivities and phases in the measurement directions (TE or transverse-electric and TM or transverse magnetic) for preliminary assessments. The gross features of these MT curves suggest a simple resistive-conductive-resistive sequence underneath variable overburden evinced by the MT response. Also, to investigate the geoelectric structure of the study area, two-dimensional modeling of the MT data was used. We choose three lines 400,500 and 900, because they are parallel to the geologic section as shown in **Fig. 2**. The survey lines undergoing the 2-D inversion have a length of 8 km and 18-24 measurements sites. The geologic section runs east-west near the center of the survey area **(Fig. 2)**.

2. Geological Setting

Minami-Noshiro is located in the northern part of Akita. This district is underlain by a thick sequence of Miocene to Pleistocene sediments and volcanic rocks. This area is an important oil field in Japan. The stratigraphic sequence of the Minami-Noshiro area is divided into Quaternary and Tertiary as shown in **Table 1**. The Tertiary sequence is divided into the Hayaguchigawa, Onnagawa, Subari Andesite, Moyasan Rhyolite, Funakawa and Tentokuji formation in ascending order. The Quaternary sediments are divided into the Sasaoka and Nakazawa formations, terrace deposits, and Alluvium[16]. The tectonic structure of Minami-

Table1 Summary of stratigraphic sequence of Minami-Noshiro area (Ozawa et al., 1984).

Geologic Age			Stratigraphy	
Quaternary	Holocene		Alluvium, Sand dune, and Terrace deposits	
Quaternary	Pleistocene		Nakazawa Formation	
Quaternary	Pleistocene		Sasaoka Formation	
Tertiary	Pliocene		Tentokuji Formation	Subari Andesite
Tertiary	Miocene	Late	Funakawa Formation	Subari Andesite
Tertiary	Miocene	Late	Moyasan Rhyolite	Subari Andesite
Tertiary	Miocene	Middle	Onnagawa Formation	
Tertiary	Miocene	Middle	Hayaguchigawa Formation	
Tertiary	Miocene	Early	Kuroishizawa formation	
Tertiary	Oligocene		Fujikuragawa Formation	

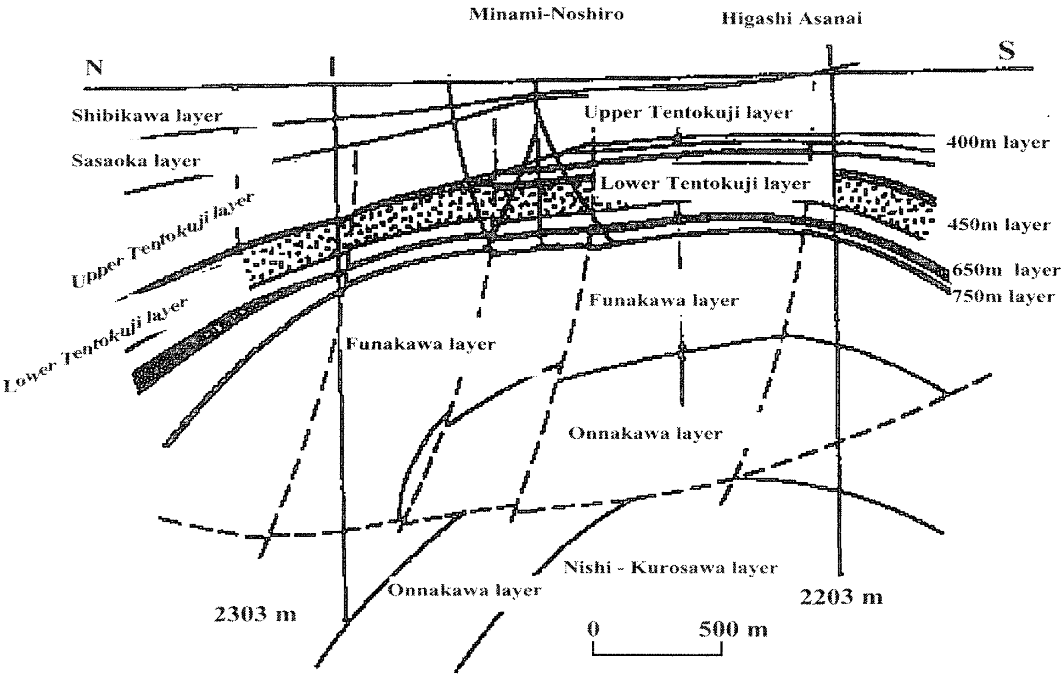

Fig. 3 The geological cross section map of Minami-Noshiro area.

Noshiro area is characterized by prevalence of NNE-trending faults and folds. Some major folds commerce to grow in the late Miocene Funakawa stage to affect the deposition, while the rest began to form afterward. Their growth has been accelerated during the Quaternary.

Most of the faults have rapidly grown through the Quaternary as well. **Figure 3** shows the geological cross section of Minami-Noshiro area. The Noshiro Thrust faults probably started to form in latest Pliocene and have rapidly accumulated their displacement through the Quaternary. On other hand, numerous strike-faults including the Moritake fault, which are distributed in the central to eastern parts of the district, were active in the early to middle Quaternary but decreased in activity through the late Quaternary. However, it is probably that the Moritake fault and other strike-faults are still active at present. The Noshiro thrust faults are one of the greatest active faults in Northeastern Honshu. Also, the Tomine fault and some other strike-faults are shown as the inferred active faults. Most of folds in the mapped area, which are closely associated with the active faults, are also considered to be active.

3. Previous studies in Minami-Noshiro area

Many studies have been carried out in Minami-Noshiro oil field. Matsuo and Minegishi[13] recognized the major geological structures of the Minami-Noshiro over thrust fault, Nakazawa syncline, and Sotooka anticline. However, some specific geological features were difficult to observe in the 2-D inversion results. Matsuo and Negi[14] made 2-D inversion of MT data and they found that the resistivity basement of the center of the area shows an uplifted structure. Minegishi et al.[15] mentioned that most problems in difficult places are caused by complex 3-D subsurface structure and insufficient wavefield sampling by irregular acquisition geometry; thus, they determined that 3-D seismic techniques offered the only possibility for successful seismic exploration in such area.

4. Magnetotelluric (MT) Method

4.1 Theoretical Background

The magnetotelluric (MT) method is a proven wavefield electromagnetic technique for deep subsurface imaging in volcanic-covered and other crystalline terrains[5, 11,20,21,1]. For plane wave source fields, in frequency domain, the horizontal electric field, E , and the horizontal magnetic field, H, are connected via a linear relationship:

$$E = ZH \tag{1}$$

Where

$$Z = \begin{bmatrix} Z_{xx} & Z_{xy} \\ Z_{yx} & Z_{yy} \end{bmatrix} \tag{2}$$

A similar relation exists between the vertical magnetic field intensity H_z and the horizontal components of the magnetic field:

$$H_z = AH_x + BH_y. \tag{3}$$

Usually, the components of the impedance tensor Z are used to calculate the apparent resistivity functions, ρ_{xy} and ρ_{yx} and the phase functions, ϕ_{xy} and ϕ_{yx} which are defined as:

$$\rho_{xy} = \frac{1}{(\omega\mu_0)}\left|Z_{xy}\right|^2, \tag{4}$$

$$\rho_{yx} = \frac{1}{(\omega\mu_0)}\left|Z_{yx}\right|^2, \tag{5}$$

The phases of the impedance tensor are

$$\phi_{xy} = \tan^{-1}\left(\frac{imZ_{xy}}{reZ_{xy}}\right) \tag{6}$$

$$\phi_{yx} = \tan^{-1}\left(\frac{imZ_{yx}}{reZ_{yx}}\right) \tag{7}$$

Where ω is the angular frequency and μ_0 is the magnetic permeability of the vacuum.

If the earth is homogeneous or horizontally layered (1-D) the impedance, phase and resistivities in xy and yx directions will be equal (i.e., resistivity changes multidimensionality, 2-D and 3-D), otherwise they will have different values for the same site for the same measurement.

4.2 1-D inversion

One-dimensional (1-D) inversion remains an important tool for interpreting MT data because there are geologic regions where lateral variation is small and 1-D interpretation is directly applicable and understanding the 1-D inverse provide a foundation for solving inverse problems in high dimensions. There are many instances, particularly at very low frequencies, when multidimensional effects may be approximated by a frequency independent static distortion and only a 1-D interpretation is necessary[23,12]. Also, 1-D inversions are routinely performed to constrain starting models for 2-D or 3-D modeling or inversion. The inversion procedure used in this paper consists of two algorithms. The first one is Occam inversion. The model produced by Occam typically consists of many layers (20 to 50). Occam inversion tries to find the smoothest possible model which produces an error with an acceptable level. The second is Marquardt inversion; it is a standard implementation of a layered-earth inversion. It requires a starting model which has the desired number of layers. It modifies the resistivities and thicknesses of the layers until it minimizes the root mean square (RMS) error between the model response and the observed data.

4.3 2-D inversion

The 2-D inversion has been used for many years to interpret the MT data. In many instances of interpretation of field data, an investigator may suspect that the geology of a field area lends itself to approximation by a model consisting of a few layers of laterally varying thickness and perhaps laterally varying conductivities. This kind of model is particularly appropriate for many areas of current interest in petroleum exploration world wide. Magnetotellurics (MT) are most often considered in petroleum exploration in cases which are difficult for seismic imaging. A near surface unit of high resistivity and velocity overlying prospective sediments above basement is the most common case. In such cases, the geometry of the base of the resistive unit and of the basement surface are primary interpretational goals.

Recent inversions have been successful in finding smoothly varying two-dimensional models fitted to magnetotelluric data[7]. The Occam inversion represents the earth as a finite element mesh which is like a "stack of bricks", each with a resistivity assigned from a palette of available values.

In this paper, the MT data (lines, 400, 500 and 900) were inverted with a 2-D Occam's inversion. The final inversion model generally fit the TE (transverse electric) data better than the TM (transverse magnetic) data because the TM mode is not sensitive to the thin vertical conductors that are well resolved by the TE mode.

5. Results of analysis of the MT soundings

5.1 Analysis of MT data

This section deals with the analysis of the data of the twelve sites (lines 400 from 401 to 412) shown in **Fig. 2**. The interpretation to study the subsurface structure of Minami-Noshiro area included the following:-

- Analysis and interpretation of impedance polar diagrams for all twelve sites.
- Analysis and interpretation of apparent resistivity and phase curves representing the TE and TM Polarizations for all twelve sites.
- Analysis and interpretation of pseudosections of apparent resistivity and phases TE and TM modes for the line 400.

Analysis of MT data begins with an estimation of the implied dimensionality of the earth. The impedance polar plots provide a measure of the MT data dimensionality[19]. The most complete strike presentation is given with the polar diagrams for all the recorded frequencies. **Figure 4** shows the polar diagram for all twelve stations. There are three curves; the outer curves are the traces of Z_{xy}, while the inside curves are the traces of Z_{xx}. The thin black line represents the regional strike direction (NE-NW) finally used in defining the two polarizations (TE and TM). For stations 407, 408, 409, 412, there is agreement in the polarization directions for all frequencies that revealed a regional strike of N30°E. Moving to other stations, we can see that the strike direction varies with frequency reflecting impedance changes with depth. Thus, for stations 401 and 411, the strike directions are almost N-S for the higher frequencies (shallower depths), rotating clockwise with depth to an E-W direction. For stations 402, 403, 405 and 410 the strike direction starts from WNW-ESE direction for shallow depths to ENE-WSW for deeper depths. The other sites are almost NNE and this is the predominant strike direction in the study area. The direction of N30°E was adopted as the strike direction for the area. Therefore, the impedance tensor was rotated to the strike direction (30°) so that xy polarization defines the TE polarization and yx polarization defines the TM polarization.

- The vector electric and magnetic fields recorded at each site were processed using Geotools software to estimate the elements of the MT impedance tensor. These impedance elements were used to determine the transverse electrical (TE mode) and transverse magnetic (TM mode) apparent resistivities and phases, which are parallel (TE) and perpendicular TM to the strike direction estimated for each frequency. Local near-surface inhomogeneities can cause pronounced static shifts of the absolute levels of the MT apparent resistivity curves[2]. **Figure 5** shows all the apparent resistivity curves with TE and TM polarizations. The apparent resistivity curves are not similar in all stations. This may be due to local surface or near-surface inhomogeneites. **Figure 6** shows the phase curves with TE and TM polarizations. Scattering of the phase curves can be due to the structure that is not truly 2-D or contributes to the degradation of the fit at some sites, as it is already explained at the presentation of the polar diagrams. Based on that information, the shift of the apparent resistivity curves is due to 3-D structure. In fact, the soundings can be classified into three groups on the basis of similarity of apparent resistivity and phase curves.

The first group includes sites 401, 408, 409 and 412. The apparent resistivities of the TE and TM modes at all four sites are similar within a common period range. The second group includes sites 402, 403, 405, 406 and 411. The last group includes sites 404, 407 and 410. In general for all sites, the apparent resistivities values decrease for periods between 0.1-10 s, which may indicate a high conductive zone underlying a resistive upper crust. For periods less than 0.1 s, the apparent resistivity data seem to indicate an increase of resistivity at lower

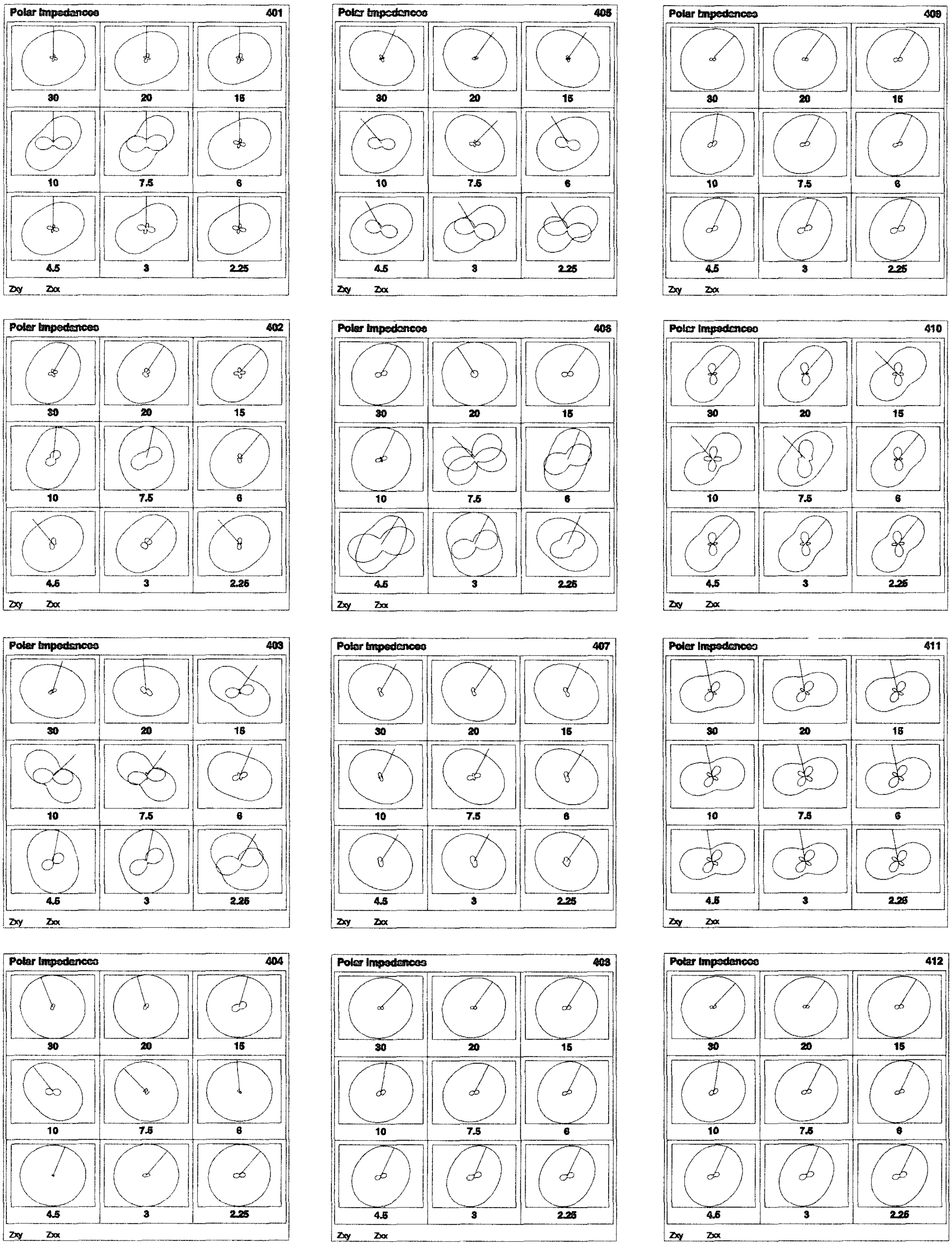

Fig. 4 Polar diagrams of the elements of the impedance tensor Z_{xy} and Z_{xx} along the relative position of the Stations of the line 400.

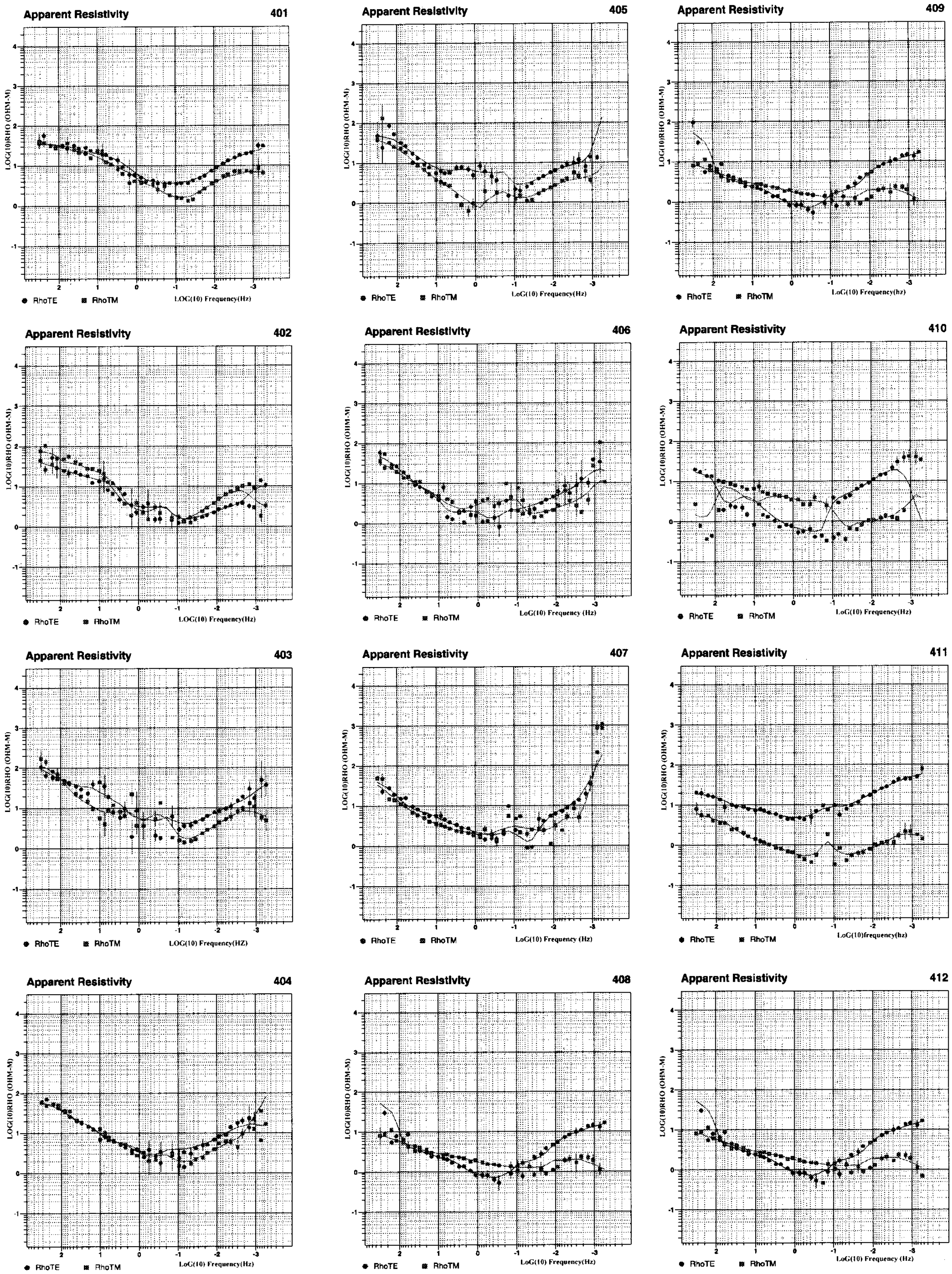

Fig. 5 The apparent resistivity of TE and TM modes at twelve sites of line 400.

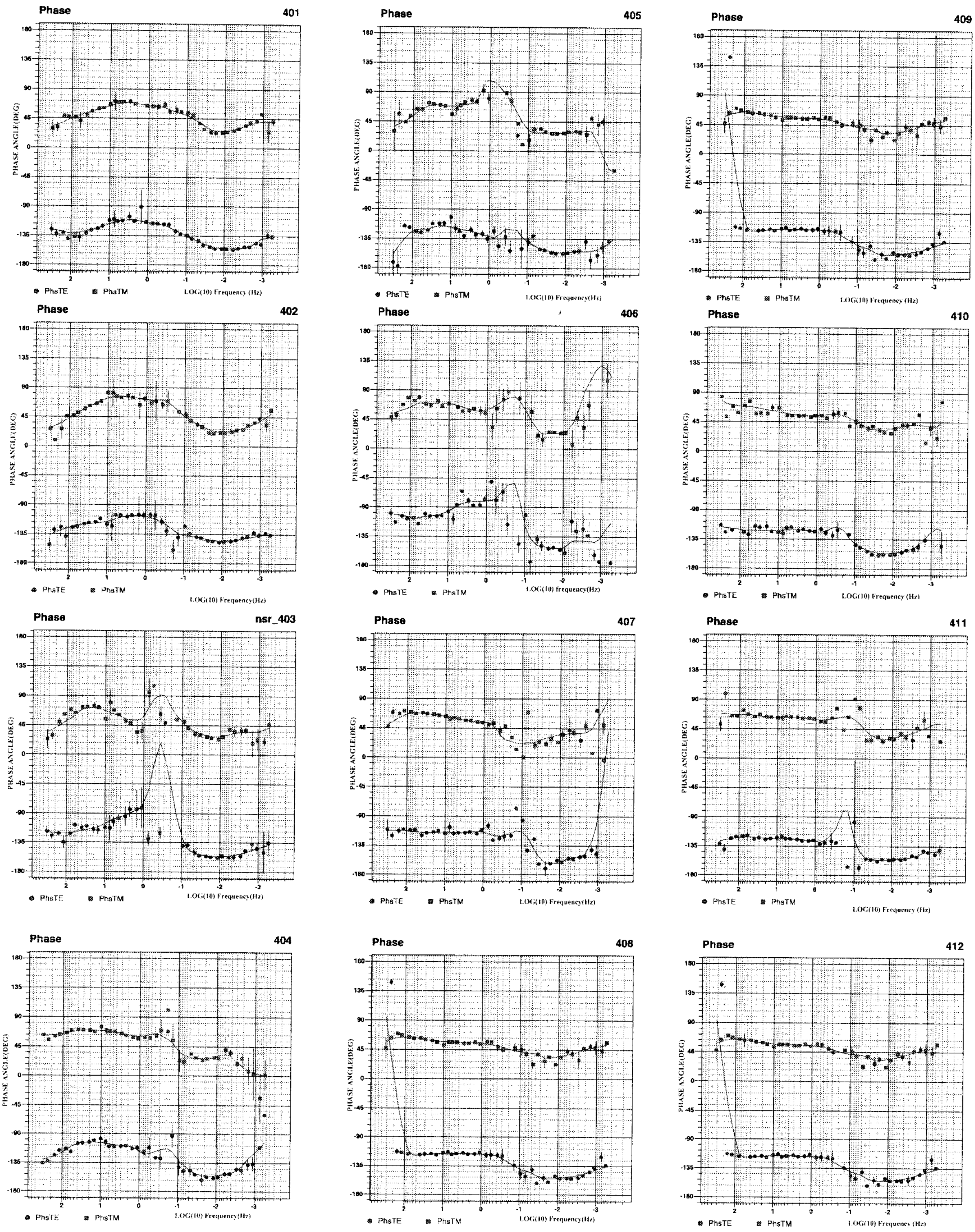

Fig. 6 The phase of the TE and TM modes at twelve sites of line 400.

depths. The observation is supported by the phase data with decreasing values. Of much greater significance may be the departure in the TE mode apparent resistivities in the period range of 10-0.001 s among the sites 408, 409, 410, 411 and 412, which may be located close to boundary fault in the study area. For this period range there is a considerable anisotropy, which may be a reflection of the lateral conductivity structure, associated with the fault in the study area. Thus, the MT results from these five sites may indicate that any electric signature of the fault exit in this area.

For comparison, **Fig. 7** shows curves demonstrating the variation in the apparent resistivity data for the three group at the twelve sites. The apparent resistivities of the TE and TM modes at all three groups are similar within a common period range. The apparent resistivities and phases (**Figs. 5, 6**) from site 411 show a considerable scatter which may be a result of culture noise for periods of about 1-100 s.

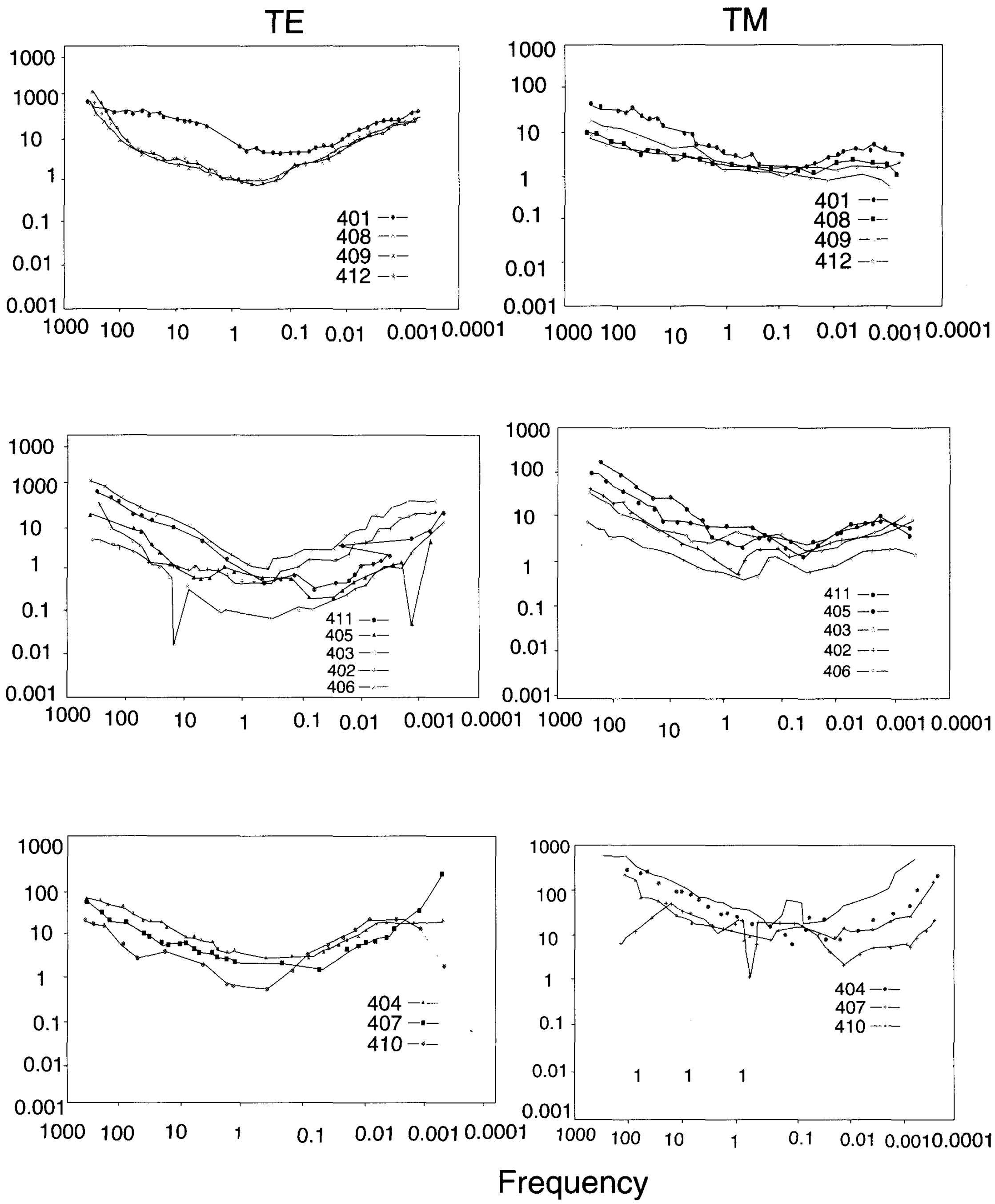

Fig. 7 The variations in the apparent resistivities of the TE and TM modes acquired on line 400.

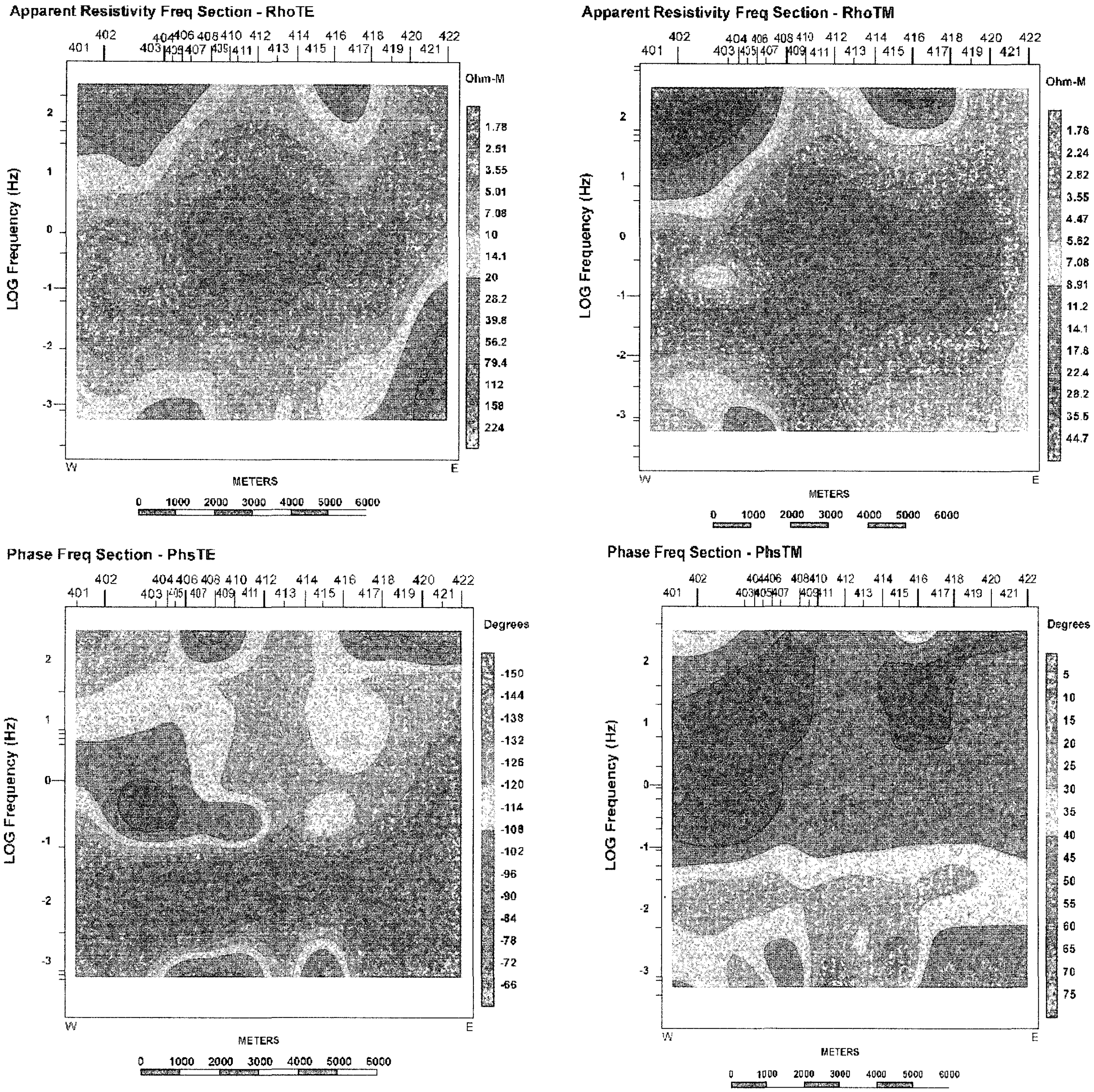

Fig. 8 Pseudosections of apparent resistivity and impedance phase acquired on the line 400.

- To get a first overview of the MT result, the measurements are introduced in the form of pseudosections, which are contour plots of MT function values with log frequency as the ordinate and distance along the profile as the abscissa[21]. Pseudosections are useful for summarizing the results concisely and for highlighting the strongest anomalies. **Figure 8** shows the data as pseudosections of the apparent resistivity and phase of the TE and TM modes of line 400. Bearing in mind the data behavior, the profile can be divided into two zones, each zone being characterized by the similar shape of the apparent resistivities and phases: -

Zone 1 in the northwestern part of the area beneath sites 401 to 408 where there is a marked increase in apparent resistivity at 0.5 s in both TM and TE polarization. This observation is supported only in phase TM. *Zone 2* beneath sites 408 to 420 where the apparent resistivities decrease continuously up to the longest periods in both polarizations, indicating a high conductivity at depth. At very shortest periods, falling apparent resistivities and high impedance phases in both modes as shown in **Fig. 8** indicate shallow low - resistivity layering in east-central portions of the area beneath thin, high resistivity cover. The conductive layers in turn overlie very resistive basement. The depth to the conductive layers appears variable. The layer is thinnest and most shallow between the center of the area according to the low phase values and steeply rising apparent resistivities. Low resistivity comes right to the surface under sites 408 to 420 coincident with the geologic structure of the area. Also, there is a sharp boundary of conductive zone at sites 408, 409, 410, 411 and 412. From the phase pseudosections of the TE and TM modes, we can observe that this area is composed of a 3-layer structure, and the resistive basement becomes gradually shallower from west to east.

5.2 One-Dimensional Inversion and electric structure

Full interpretation of the magnetotelluric results will require a detailed analysis of possible distortions in the data[9] and, at the very least, two-dimensional modeling and inversion. However, certain inferences concerning the electrical structure, especially in the relatively near-surface, may be obtained from one-dimensional modeling and inversion. The apparent resistivities and phases used in this modelling are those calculated from the determinant impedance. This parameter is invariant with rotation of the axial system and may be less sensitive to the local three-dimensional structure[10].

In this study, two different techniques have been used for producing one-dimensional models, which give an indication of the electrical structure beneath the various regions in the study area: Occam's inversion[6] which produces models which are maximally smooth in resistivity structure and Marquardt inversion.

Results of modelling and inversion of the invariant responses at site 401 using the two techniques are shown in **Fig. 9**. At this site, the apparent resistivity and phase responses for both polarizations are quite similar up to frequencies 1000 Hz (**Figs. 5 and 6**). This site is located on the western side near the Japan Sea as shown in **Fig. 2**. Thus, one-dimensional modelling may give a good indication of the structure at site 401 to considerable depths. The Occam inversion fits the data set with an RMS misfit (calculated from the mean square misfit normalized by the variance of the estimates) of 0.6. An RMS misfit of 0.1 is generally regarded as providing a satisfactory fit to the data while avoiding the danger of overfiting. In this instance, because of the large statistical uncertainties in the long period estimates, relaxing the RMS misfit to 1.0 does not provide a good fit to the phase data. Both models indicate very clearly the existence of a good conductor of resistivity around 10 ohm-meters at a depth of between 600 and 1200 m.

This indication of a good conductor at depth is given firm support by the smooth modelling of the invariant responses at the other sites. The Occam inversions for all eleven sites are shown in **Fig. 10**. Although the data are slightly more scattered at some sites than at others, the indications of conductive structure at similar depths are unambiguous. From **Fig. 10** a conductive region exists generally beneath sites as follows:

- Site 402 with average values of 1000 m and 30 Ωm.
- Site 403 with average values of 1200 m and 80 Ωm.
- Site 405 with average values of 500 m and 30 Ωm.
- Site 406 with average values of 1200 m and 140 Ωm.
- Site 411 with average values of 1000 m and 30 Ωm.

Local differences in very near-surface resistivity do appear to exist and there is also a suggestion of a second conducting layer at around 1-2 km depth.

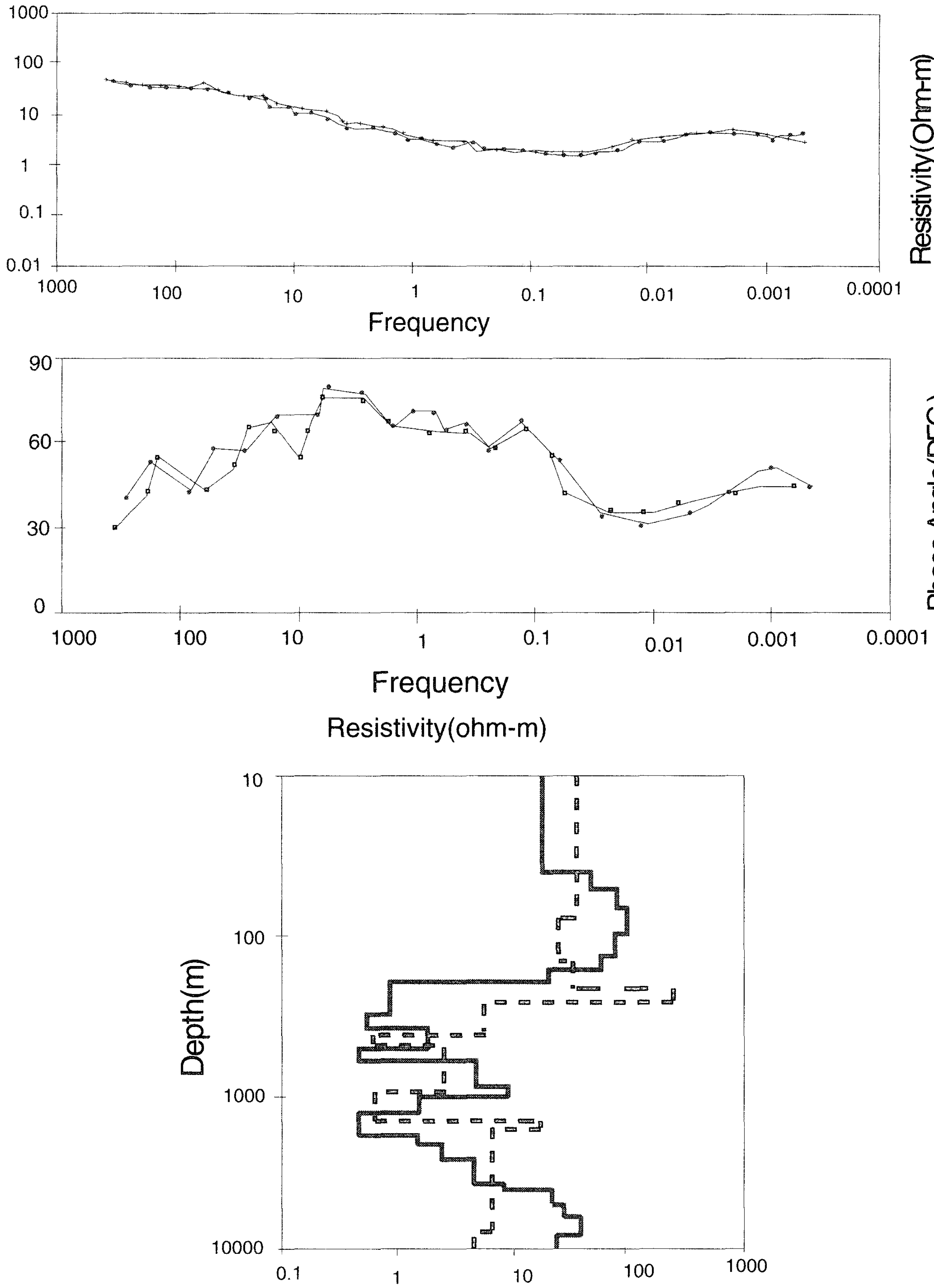

Fig. 9 One-dimensional inversion of MT data at site 401(Solid line: Occam smooth inversion, dotted line: Marquardt inversion.

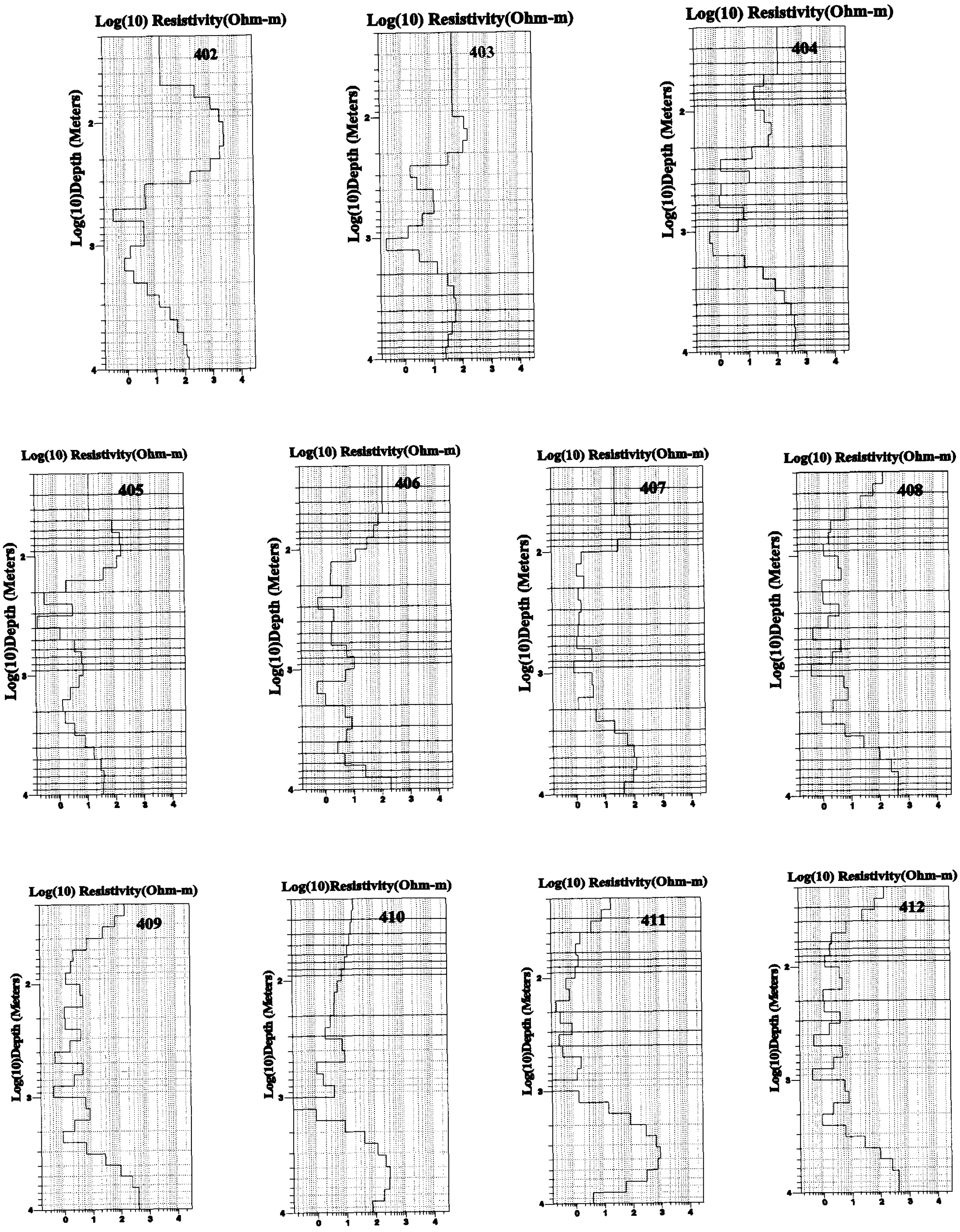

Fig. 10 Occam smooth inversions of MT data at eleven sites.

5.3 Comparison between 1-D models and well logging data

Fortunately, there are two electric well logs at Higashi Asanai and Sotooka sites. Therefore, the resistivity logs can be used as an aid for interpretation of the MT results. To evaluate MT method as a reconnaissance tool, we made comparison between the results of 1-D models and the resistivity log data. **Figure 11** depicts the 1-D inversion models at Higashi

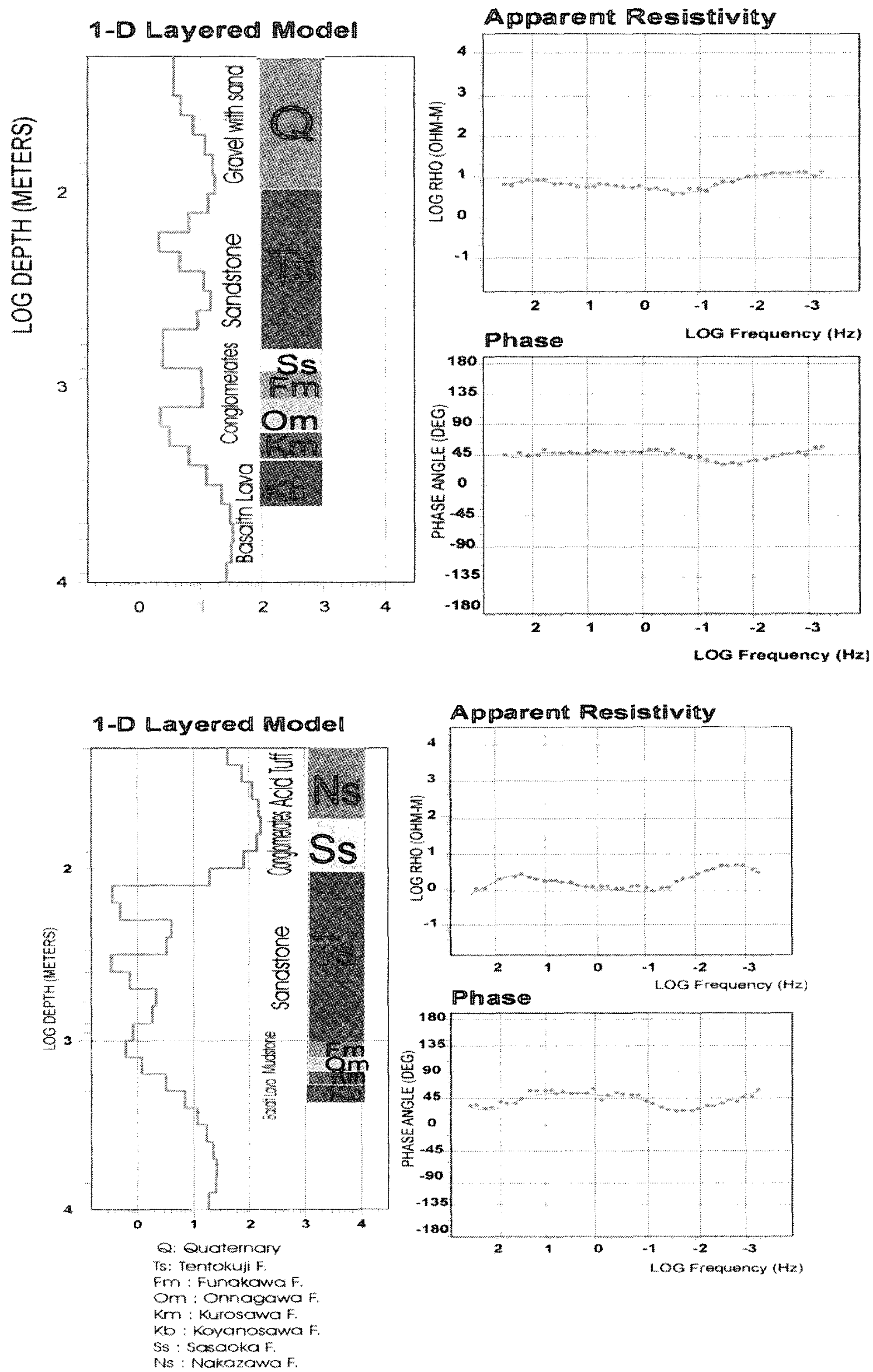

Fig. 11 1-D Occam inversion of MT data with well logging data at Higashi Asanai and Sotooka sites.

Asanai and Sotooka sites that have well logs available for comparison. The inversion on Higashi Asanai was run with the resistivity and the thickness composed of the fourteen layer. The major resistivity units of the electric log agree with the 1-D model. The low resistivity zone at 400 and 500 m depth is sandstone, and more resistive zone correlated to mudstone. From **Fig. 11**, it is shown that there is a good agreement between MT interpretation and well logging data.

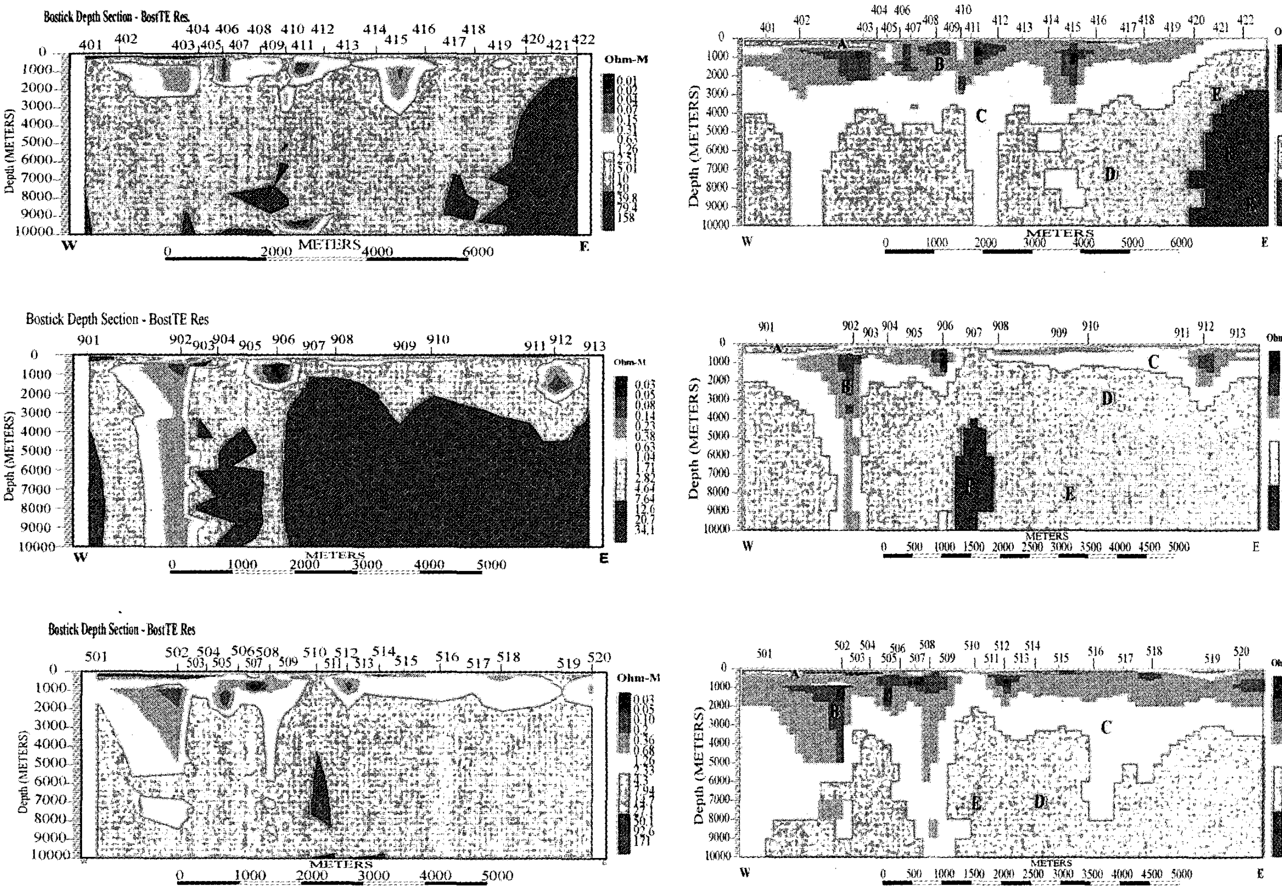

a **b**

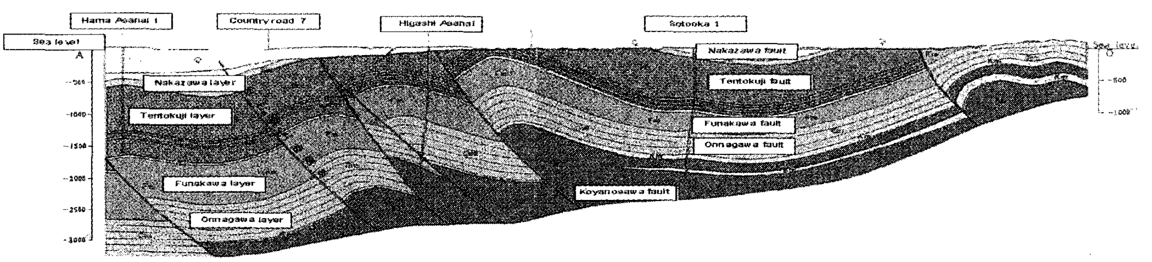

c(after Ozawa et.al.,1984)

Fig. 12 Two-dimensional inversion resistivity models along lines 400, 900 and 500 (a) the sections of Bostick depth (b) 2-D results of lines 400, 900 and 500 from north to south and (c) the geological cross section.

6. Two-dimensional inversion and interpretation

The MT data of lines, 400, 500 and 900 were inverted with a 2-D Occam's inversion. The gross structure of the model was derived from fitting the TE data.

Figure 12 shows the two-dimensional resistivity structure for the three profiles of lines 400,500 and 900. The Bostick depth sections using TE mode **(Fig. 12a)** and the depth responses of 2-D resistivity for TE mode are also presented **(Fig. 12b)**. Both resistivity sections were obtained from observed data for TE mode. A geological cross-section along the MT profiles (Ozawa et al., 1984) was used to highlight the features of the inversion results.

The major geoelectric structures in the final models with labeled A-F are discussed below:-

- In the shallow part of the line 400, there is a small anomalous zone (< 40 Ωm), which show moderately high resistivity at 0-2 km depth (labeled A). We can see this zone also in lines 900 and 500.
- There is a conductive zone in line 400 (<3 Ωm) at a depth around 0.5 to 3.5 km (labeled B) in different places from east to west of the area. In line 900, this zone is limited and there is a sharp boundary to the conductive zone at site 902, while in line 500, this zone is much bigger and found in many parts of the line. This zone is supported by the observations in the depth sections, which show moderately low resistivity at 0.5-2 km depth.
- There is another conductive zone in line 400(<10 Ωm) at a depth around 0.5 to 10 km (labeled C) in different places from east to west of the area. This observation is found in lines 900 and 500.
- There is a resistive zone in line 400(<40 Ωm) at depth around 4 to 10 km (labeled D) in different places from east to west of the area. We can see this resistive zone in lines 900 and 500 at different areas of the lines.
- There is more resistive zone in line 400(<250 Ωm) at a depth around 4 to 10 km (labeled E). In line 900, this zone is very limited at a depth 4.5 to 10 km, while it does not appear in line 500.
- The final resistive zone appear only in line 400 (<800 Ωm) at depth around 8 to 10 km (labeled F).

Comparison between the geologic cross-section and the 2-D geoelectrical models shows that between the depths of 0 and 0.4 km, the 2D geoelctrical models **(Fig. 12b)** reflect both vertical and horizontal resistivity variations consisted of high values. On the other hand, the shallow parts of the model have high resistivity values in the upper parts of these areas. These areas correspond to the Quaternary, Koyanosawa formation, which consists of basaltic lava, mudstone, and acidic pyroclastics rock of the Miocene. Between the depths of 0.5 and 3 km, the 2-D geoelectrical models reflect low resistivity values, these areas correspond to Tentokuji formation which consists of siltstone, sandstone and acid tuffs.

Conclusions

The major objective of the present study is to investigate the structure of Minami-Noshiro area from MT soundings. The MT survey in the Minami-Noshiro oil field brought meaningful results. The interpretation to study the subsurface structure of Minami-Noshiro area include the analysis and interpretation of impedance polar diagrams for all twelve sites, analysis and interpretation of apparent resistivity and phase curves representing the TE and TM Polarizations for all twelve sites, analysis and interpretation of one-dimensional Occam and Marquardt inversions for all twelve sites along the line 400. The most interesting and unique features determined by the MT analysis are the low resistivity zone (conductive one) beneath all the sites as shown in the apparent resistivities curves and the regional strike direction of the study area is N 30° E. Also, the crustal structure below Minami-Noshiro comprises a complex 2-D or even 3-D geoelectric domain of interesting conductive zones and resistive blocks. The results from this study show the magnetotelluric method can provide valuable information about electrical conductivity and the crustal structure of Minami-Noshiro area and the existence of number of low-resistivity zones in the area is undoubtedly the most important feature found in this study. These results are supported by the results from pseudosections of apparent resistivity and phase of TE and TM. There is a shallow low - resistivity layering in east-central portions of the area beneath thin, high resistivity cover.

From the comparison between the 1-D results and well logging data, there is a good agreement between MT interpretation and electrical well logging data and the MT resistivity models can be used, in conjunction with log data, to determine the location of conductive zones.

Finally, the original motivation for this work was to present the results of regional deep resistivity structure along three profiles to contribute in the understanding of the resistivity structure from MT data. The geological cross-section was used to highlight the features of the geoelectrical 2-D resistivity models. The most interesting result is the existence of large conductive zones and there is reasonable agreement in the results between the geological cross section and 2D resistivity models. Our results are in agreement with the inversion results of Matsuo and Negi (1999) on the same data set using different inversion algorithms.

Acknowledgments

We are grateful to Teikoku Oil Company and Japan National Oil Company (JNOC) for their permission to use MT data and publish this paper. We also grateful to Mr. Tateyuki Negi for his helpful discussions. We are indebted to all of the staff of the Exploration Geophysics Laboratory of Kyushu University for their contribution and support during this work.

References

1) Bai, D. B., Meju, M.A., Liao, Z., 2001. Magnetotelluric images of deep structure of the Rehai geothermal field near Tengchong, southern China. Geophys. J. Int. 147, 677-687.
2) Beamish, D., and Travassos, J., 1992. A study of static shift removal from magnetotelluric data: J. Appl. Geophys. 29, 157-178.
3) Berdichevsky, M. N., Dmitriev, V. I., 1976. Basic principles of interpretation of magnetotelluric curves, in *Geoelectric and Geothermal studies*, pp.165-221, ed. A. Adam, KAPG Geophysical Monograph, Akademiai Kaido, Budapest.
4) Chien C., Chow C., 1998. Preliminary result of magnetotelluric soundings in the fold-thrust belt of Taiwan and possible detection of dehydration.
5) Christopherson, K.R., 1991. Application of magnetotelluric to petroleum exploration in Papua New Guinea; a model for frontier areas. Geophysics: The leading Edge of Exploration 10, 21-27.
6) Constable, S.C., Parker, R.L., and Constable, C.G., 1979. Occam's Inversion: A practical algorithm for generating smooth models from electromagnetic sounding data. Geophysics, 52, 289-300.
7) deGroot-heldin, C. and Constable, S., 1990). Occam's inversion to generate smooth two-dimensional models from magnetotelluric data, Geophysics 55 1613-1624.
8) Fischer, G., Schneeg, P. A., Peguiron, M. and Le Quing, B.V., 1981. An analytic one-dimensional magnetotelluric inversion scheme. Geophys. J. R. Astron. Soc., 67:257-278.
9) Groom, R.w. and Bailey, R.C., 1989. Decomposition of magnetotelluric impedance tensor in the presence of local three-dimensional galvanic distortion. J. Geophs. Res., 94:1913-1925.
10) Ingham, M. R., 1988. The use of invariant impedance in magnetotelluric interpretation, Geophys. J. R. astr. Soc., 92, 165-169.

11) Jones, A. G., 1993. Electromagnetic images of ancient and modern subduction zones. Tectonophysics 219, 29-45.

12) Larson, J. C., 1977. Removal of local surface conductivity effects from low frequency mantle response curves: Acta Geodaet., geophys.et Montanist. Acad. Sci. Hung., 43, 897-907.

13) Matsuo, K., and Minegishi, M., 1998. The three dimensional magnetotelluric survey for hydrocarbon exploration on the over thrust area in Japan: *Electromagnetic Induction Workshop*, Romania

14) Matsuo, K., and Negi, T., 1999. Oil exploration in the difficult Minami - Noshiro area. Part 2: magnetotelluric survey. *The Leading Edge*, Vol. 18, No.12, 1411-1413.

15) Minegishi, M., Tanaka, H., and Nakagami, K., 1999. Oil exploration in the difficult Minami - Noshiro area. Part 1: 3-D seismic. *The Leading Edge*, Vol.18, No.12, 1408-1410.

16) Ozawa, A., Ikebe, Y., Hirayama, J., Awata, Y., and Takayasu, T., 1984. Geology of the Noshiro district. Geological Survey of Japan, 83- 91.

17) Park, S. W., Livelybrooks, D. W., 1989. Quantitative interpretation of rotationally invariant parameters in magnetotelluric, Geophysics, 54, 1483-1490.

18) Ranganayaki, R. P., 1984. An interpretation analysis of magnetotelluric data, Geophys. 49, 1730-1748.

19) Reddy, I. K., Rankin, D., Phillips, R. J., 1977. Three-dimensional modelling in magnetotelluric and magnetic variational sounding. Geophysics Journal of the Royal Astronomical Society, Vol. 51, P. 313-325.

20) Simpson, F. L., Haak, V., Khan, M.A., Sakkas, V., Meju, M.A., 1997. The KRISP-94 magnetotelluric survey of early 1995: first results. Tectonophysics 278, 261-271.

21) Simpson, F., 2000. A three-dimensional electromagnetic model of the southern Kenya Rift: departure from two-dimensionality as a possible consequence of a rotating stress field. J. Geophys. Res. 105, 19321-19334.

22) Vozoff, K. (Ed), 1986. Magnetotelluric methods: Geophys. Reprint Series, Vol. 5, Soc. Explor. Geophysics.

23) Weidelt, P., 1972. The inverse problem of geomagnetic induction: Z. Geohysics. 38, 257-289.